Spectrochimica Acta Part A: Molecular and Biomolecular Spectroscopy xxx (xxxx) xxx

Contents lists available at ScienceDirect

Spectrochimica Acta Part A: Molecular and Biomolecular Spectroscopy

journal homepage: www.elsevier.com/locate/saa

Original synthesis and spectroscopic study of thiophene triazine derivatives with enhanced luminescence properties

Alysson Duarte Rodrigues [a, c], Nathalie Marcotte [a, c], Françoise Quignard [a], Stefano Deabate [b, c], Mike Robitzer [a, c, *], Dan A. Lerner [a, c, **]

[a] ICGM, Univ Montpellier, ENSCM, CNRS, Montpellier, France
[b] Institut Européen des Membranes, IEM – UMR, 5635, ENSCM, CNRS, Univ Montpellier, Montpellier, France
[c] Ecole National Supérieure de Chimie de Montpellier, 240 Avenue du Professeur E. Jeanbrau, 34296, Montpellier Cedex 5, France

ARTICLE INFO

Article history:
Received 14 July 2019
Received in revised form
21 October 2019
Accepted 24 October 2019
Available online xxx

Keywords:
Thiophene
Oligothiophene
Triazine
Palladium catalyzed C–H arylation
Fluorescence
Fluorescent label

ABSTRACT

A straightforward access to π-conjugated oligothiophenes bearing amino-rich groups was developed. Palladium-catalyzed C–H arylation applied in the main step of the synthesis allowed to couple 2-thiophenecarbonitriles and aryl bromides with moderate to excellent yields (35–93%). Then, to improve their basic fluorescence properties, these compounds were transformed into their 2,4-diamino-1,3,5-triazine derivatives, also with good to excellent yields (74–98%). UV-Visible absorption and fluorescence studies identified a strongly emissive molecule (fluorescence quantum yield: $\Phi_F = 0.78 \pm 0.05$), which could find use in sensors for applications in biology and in material chemistry. We observed an antagonistic effect in the spectroscopic properties of oligothiophenes bearing 2,4-diamino-1,3,5-triazine, resulting in improved absorptive and emissive properties for more constrained structures having shorter oligothiophenes chains.

1. Introduction

Oligothiophenes (OTs) have proven to be one among the most promising functional materials for a wide range of applications. The most notable properties of these compounds are related to their electrical conductivity and light emitting characteristics sensitive to environmental stimuli [1]. Both color and conductivity changes, induced by the same twisting mechanism of their mostly linear molecular structures, have been intensely studied in conducting films for electrochromics [2–4] or in solution for sensing applications [5–7].

2,4-Diamino-1,3,5-triazines (DATs) are polar, nitrogen-containing heterocycles widely used in many domains of chemistry. They are involved in the development of conducting films [3-4], fire resistant resins [8], polymers [9], therapeutic drugs [10], herbicides [11], gas storage [12] and some DATs containing catalysts benefit from their nitrogen-rich content and high stability [13].

As discussed in our former work, the fluorescence properties of OT-DAT compounds might find applications in biology as fluorescent sensitizers, due to their activity towards Prion proteins [14]. The synthesis of OTs bearing amino-rich groups is a challenge due to their lack of solubility in the most of laboratory common solvents, what obviously hinders purification. To catalytically couple thiophenes, conventional cross-coupling reactions as those of Stille, Kumada, Negishi and Suzuki are most frequently used [6,15]. But such protocols are often time-consuming and require expensive and/or toxic organometallic catalysts (e.g. Sn-based).

In order to improve the synthesis of OTs bearing amino-rich groups, we have developed an adapted Fagnou's approach [16–18] using a palladium-catalyzed C–H arylation to promote C–C bond formation. This pathway allows largely increased reactivity in the concerted metalation deprotonation mechanism (CMD) of the reaction between 2-thiophenecarbonitrile and aryl bromides (Scheme 1). The final compounds synthesized by this approach have been fully characterized and their basic absorption and photoluminescence properties have been determined and compared.

2. Results and discussion

2.1. A new and efficient synthetic route for the preparation of OT-DAT compounds

The aryl bromide precursors (Scheme 2 – **left side**) were commercially available or prepared according to literature data

* Corresponding author. ICGM, Univ Montpellier, ENSCM, CNRS, Montpellier, France.
** Corresponding author. Ecole National Supérieure de Chimie de Montpellier, 240 Avenue du Professeur E. Jeanbrau, 34296, Montpellier Cedex 5, France.
E-mail addresses: mike.robitzer@enscm.fr (M. Robitzer), dan.lerner@enscm.fr (D.A. Lerner).

https://doi.org/10.1016/j.saa.2019.117708
1386-1425/

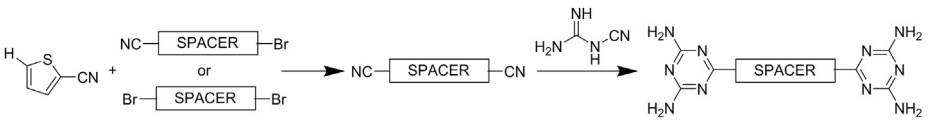

Scheme 1. Schematic pathway for the synthesis of thiophene diaminotriazine derivatives.

[18]. 5-bromothiophene-2-carbonitrile (**1**) was obtained by reacting 2-thiophenecarbonitrile with bromine (Br_2) and N-bromosuccinimide (NBS) in a solvent mixture of acetic anhydride / acetic acid 50/50 (v/v %) during 14 h at room temperature. The final product was then isolated by column chromatography using cyclohexane as eluent. The 5,5′-dibromo-2,2′-bithiophene (**2**) was obtained in an acetic acid / chloroform 50/50 (v/v %) solvent mixture at room temperature using NBS as brominating agent. The final product was isolated by successive recrystallizations in acetone. All compounds have been characterized by ^{1}H and ^{13}C NMR, UV-Vis, ATR-FTIR, HRMS (see 4-experimental part).

OTs bearing nitrile groups (**3**–**6**) (Scheme 2 - **middle**) were obtained in a single step by the palladium-catalyzed C–H arylation pathway reacting 2-thiophenecarbonitrile and the respective aryl bromides.

The palladium-catalyzed C–H arylations (**step i**, Scheme 2) were monitored by thin layer chromatography (TLC) and UV-Vis absorption spectroscopy and were stopped when no more reactivity was detected (after around 48h). The N,*N*-dimethylacetamide/toluene 50:50 (v/v %) solvent mixture provided the best solubility at 110 °C among all solvents tested and was chosen as the standard solvent mixture for all tries.

In the presence of tetrakis-(triphenylphosphine)palladium(0), K_2CO_3 and pivalic acid, the expected products (**3**–**6**) were synthesized in moderate to excellent yields (35–93%). Purifications were carried out by successive recrystallizations in appropriate solvents (**3**, **4** and **6** in 1-butanol and **5** in toluene at room temperature).

Yields were observed to improve with the number of reactive sites (-Br) of the precursor aryl bromides and the OT chain length. This suggests phenyl-bromide intermediates to be more reactive than thienyl ones. Results lead to the following reactivity scale in terms of isolated yields: 1,3,5-tribromobenzene > 5,5′-Dibromo-2,2′-bithiophene > 2,5-dibromothiophene > 5-bromothiophene-2-carbonitrile.

Further investigations carried out by GC-MS at the end of reactions revealed lower contents of mono- (<1%) and di- (2.4%) arylated intermediates when 1,3,5-tribromobenzene was used as aryl bromide. These results contrast with the higher contents of mono-arylated intermediates found using 5,5′-dibromo-2,2′-bithiophene (13%) and 2,5-dibromothiophene (31%) respectively. Although the better electronic delocalization of benzene seems to favor the CMD mechanism, thienyl bromides allow good conversions when less deactivating groups are substituted at the C2-position of the thiophene, giving to the following reactivity scale: 5′-bromo-thiophene > -Br > –CN.

The transition state (TS) involving both substrates in the palladium-catalyzed C–H arylations was consistent with the presence of a pivalate anion assisting the deprotonation of 2-thiophenecarbonitrile in C5 position and favoring its oxidative addition in the palladium catalyst [16-17]. The desired products were obtained by a reductive elimination step [18].

The diaminotriazine derivatives **3a**-**6a** (Scheme 2 – **right side**) were easily obtained by cycloaddition between the nitrile precursors (**3**–**6**) and 2-cyanoguanidine. Reactions were carried out in DMSO at 80 °C using KOH as base, and the pure compounds (**3a-6a**) were isolated following successive recrystallizations in THF. The compounds solubility decreased with the addition of the DAT groups.

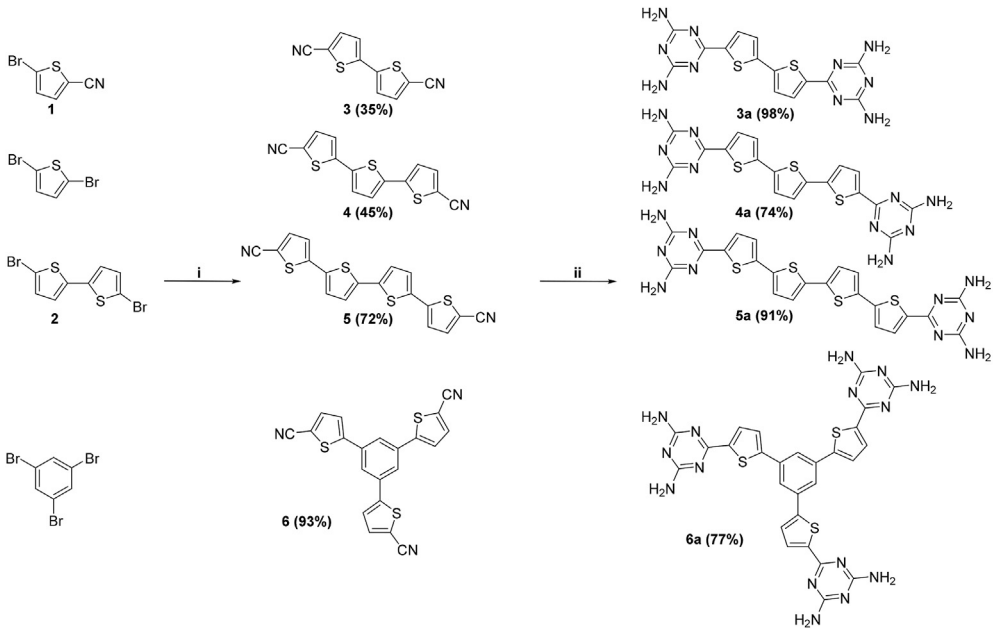

Scheme 2. Molecular structure and synthesis yields (%) of OTs bearing nitriles and diaminotriazines (**3**–**5** and **3a-5a**) or phenylthiophene bearing nitriles and diaminotriazines (**6** and **6a**): **(i)** (3 eq.) 2-thiophenecarbonitrile, (4 mol %) $Pd(PPh_3)_4$, (1.5 eq.) K_2CO_3, (0.15 eq.) pivalic acid, N,*N*-dimethylacetamide/toluene 50/50 (v/v %), C: 0.23 M, 110 °C, 48h and (**ii**) (3 eq.) 2-cyanguanidine, (1 eq.) KOH, DMSO C: 0.1 M, 80 °C, 16h. All amounts (eq.) are calculated according to the number of precursor reactive sites ((**i**) -Br and (**ii**) –CN).

Please cite this article as: A.D. Rodrigues et al., Original synthesis and spectroscopic study of thiophene triazine derivatives with enhanced luminescence properties, Spectrochimica Acta Part A: Molecular and Biomolecular Spectroscopy, https://doi.org/10.1016/j.saa.2019.117708

2.2. Infrared spectroscopy

Fig. 1 compares normalized infrared (ATR-FTIR) spectra of compounds **3**–**6** and **3a-6a**. As expected, spectral changes are mostly observed in the spectral domains of nitrile $(C{\equiv}N)_{str}$ and amine $(N{-}H)_{str}$ stretching vibrational modes (2260-2210 and 3400-3250 cm^{-1} ranges respectively) as well as in the region of the $(N{-}H)_{bend}$ bending mode (1650-1580 cm^{-1}). Compounds **3**–**6** display the characteristic bands due to the $(C{-}H)_{str}$ and$(C{-}H)_{bend}$) modes of thiophenes, at 3000-2850 and ~1400 cm^{-1} respectively. The nitrile function can be identified with the narrow band at 2212 cm^{-1} due to the $(C{\equiv}N)_{str}$ mode. Spectra of compounds **3a-6a** show the disappearance of the latter and the appearance of the primary amine bands at 3327 cm^{-1} ($(N{-}H)_{str}$ mode) and 1647 cm^{-1} ($(N{-}H)_{bend}$). The aromatic DATs are identified by the presence of the $(C{-}N)_{str}$ mode typical of heterocycles at 1379 cm^{-1}.

2.3. Electronic spectroscopy

The photo-physical properties of the different compounds were firstly investigated by UV-Visible absorption spectroscopy, in the range of 200–700 nm. The emission properties were then characterized by excitation at different wavelengths Absorption and emission spectra of compounds (**3**–**6**) and their DAT derivatives (**3a-6a**) (Figs. 2 and 3 respectively) were all obtained in air equilibrated DMSO solutions and at room temperature (23 °C ± 2 °C). Relevant data are summarized in Table 1. Emission spectra stayed unchanged whatever the excitation wavelength.

In view of the potential use of some of these compounds in organic semiconductors, for which the knowledge of the band gap is essential, we estimated E_g (Table 1) in addition to the value of the 0-0 energy transitions. E_g values were obtained from the absorption edge of the lowest energy band of the UV-visible spectrum, as described for instance in the work of Bhadwal [21] or Costa [22]. The two sets of data, E_{00} *and Eg*, based on purely optical parameters of individual molecules, were expected to give nearly identical values, even if approximated for E_g.

It should then be point out that the 0-0 gap of a molecule can be computed with all the desired accuracy whereas obtaining the true values of *Eg* would require the theory of electronic band structures specially derived for crystals with a lattice periodicity. So, E_g values may be very different, depending on the molecules packing and orientation (see Ref. [23] for more details about this issue). Ideally the E_g notation for a single molecule should be renamed "the optical band gap" with a symbol like OE_g or $E0\text{-}0_g$ for instance to avoid confusion. Experimentally, the actual value of *Eg* may be obtained by various methods such e.g. running reflectance spectra, cyclic voltammetry, etc. [23].

2.3.1. UV-vis spectroscopy

The absorption maxima of the different compounds are observed to red-shift with the increase of the chain length of oligothiophenes i.e. λ_{max} bithiophenes (**3** and **3a**) < λ_{max} terthiophenes (**4** and **4a**) < λ_{max} quaterthiophenes (**5** and **5a**) (Fig. 2). As shown by E_{00} (eV) values (Table 1), this evolution results from the progressive reduction of the HOMO-LUMO energy gaps. Due to their specific structures, tripodes (**6** and **6a**) exhibit higher energy band gap values (3.9 eV and 3.6 eV for **6** and **6a** respectively), with λ_{max} red-shift when going from nitrile (**6**) to the DAT derivative (**6a**). These compounds, with more compact molecular structures, might find applications in material chemistry as insulators for instance.

Nitrile derivatives (**3**–**5**) exhibit the increase of the molar absorptivity with the increase of the OT chain length: on average of 7700 L mol^{-1} cm^{-1} per added thiophene. Furthermore, the transformation of **3** into **3a** by the double cycloaddition reaction increases the molar absorptivity up to about 28000 L mol^{-1} cm^{-1}. Compound **3** presents $\varepsilon = 9860$ L mol^{-1} cm^{-1} and **3a** $\varepsilon = 37910$ L mol^{-1} cm^{-1}, which means that compound **3a** absorbs light 3.8 times more than compound **3**. According to the above, direct observations for the **3**–**5** serie and the **3**-**3a** transformation, one would expect **3a**-**5a** DAT derivatives to exhibit the same ε increase trend. On the contrary, the molar absorbivity of compounds **3a**-**5a** decreases with the increase of the OT chain length. Compound **3a** presents ε = 37910 L mol^{-1} cm^{-1}, **4a** ε = 36200 L mol^{-1} cm^{-1} and **5a** ε = 30150 L mol^{-1} cm^{-1}. This is the hint of an antagonistic phenomenon affecting the absorption properties of DAT derivatives.

Although tripods **6** and **6a** do not present the same molecular structures as OT derivatives, we observe the same decrease of the ε values in the **6** → **6a** transformation (from 39920 L mol^{-1} cm^{-1} to 26630 L mol^{-1} cm^{-1}). This confirms that the antagonistic effect brought by the DAT function is also found in molecules with less conjugated systems and different molecular structures.

2.3.2. Fluorescence

The Fig. 4-A and B compare fluorescence brightness of compounds **3**–**6** and **3a-6a** respectively, in DMSO solution. Perylene is used, as standard (**P**, $\Phi_F = 0.78 \pm 0.02$ in DMSO). Fig. 4-C shows the

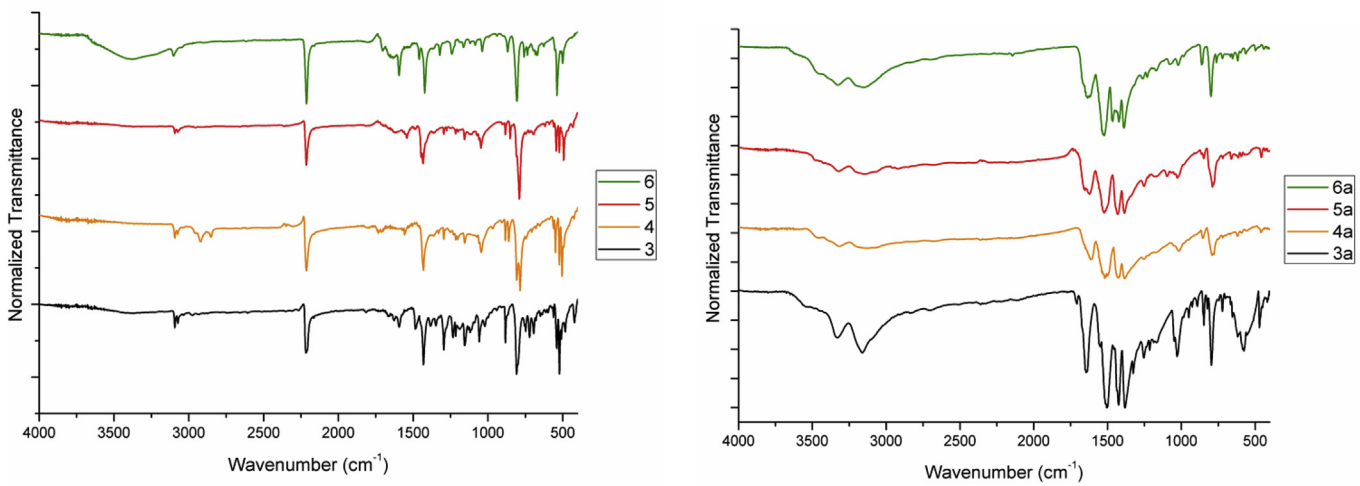

Fig. 1. ATR-FTIR spectra of compounds (**3**–**6**) (left) and (**3a-6a**) (right).

Please cite this article as: A.D. Rodrigues et al., Original synthesis and spectroscopic study of thiophene triazine derivatives with enhanced luminescence properties, Spectrochimica Acta Part A: Molecular and Biomolecular Spectroscopy, https://doi.org/10.1016/j.saa.2019.117708

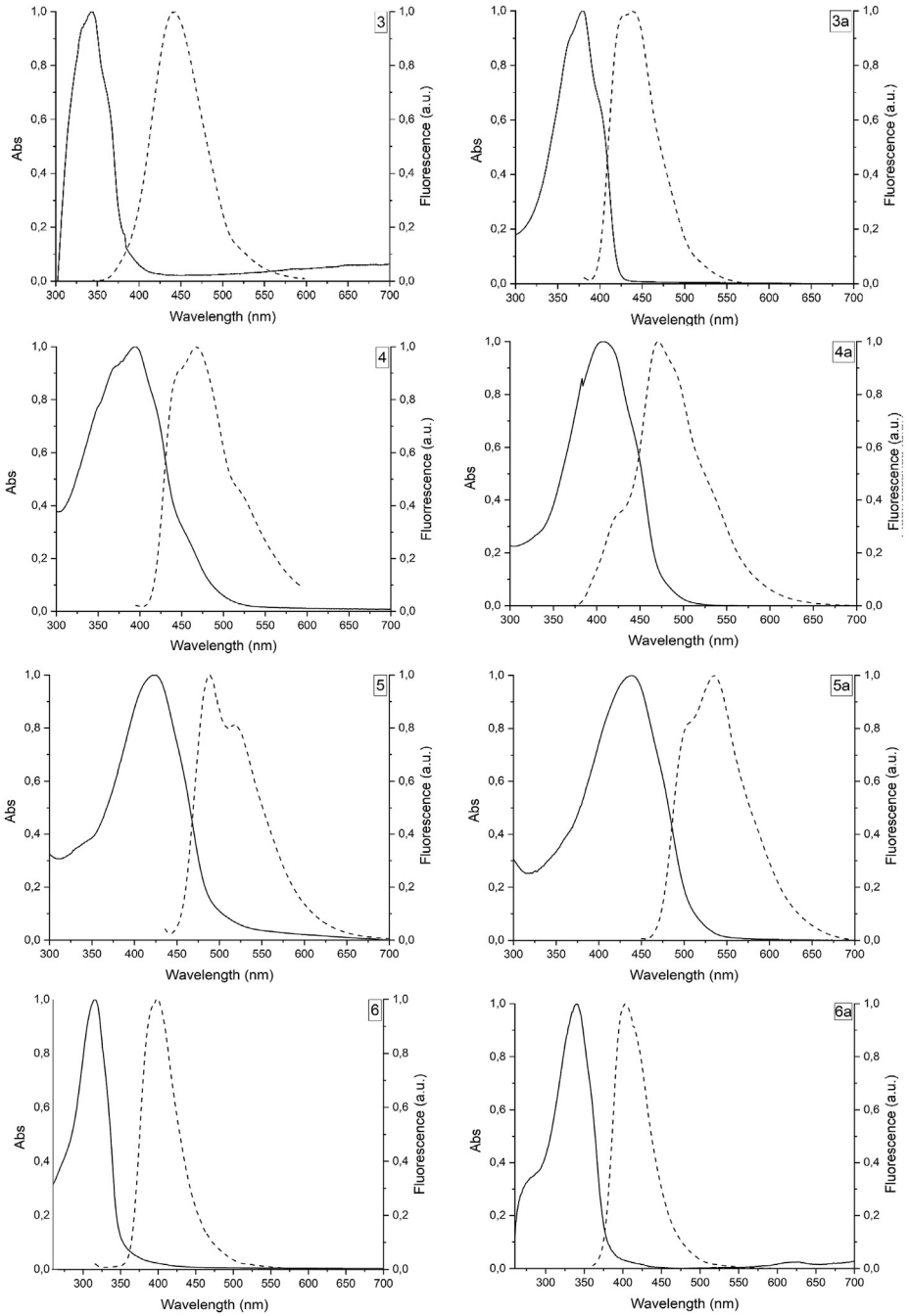

Fig. 2. Normalized absorption (solid line) and emission (dashed line) spectra of compounds **3**–**6** and **3a-6a** in air equilibrated DMSO solutions at T_{room}.

colored compounds **3a-6a** at the solid state. A brightness increase is observed for all compounds in DMSO solutions when going from nitriles to DAT derivatives. The emitted colors shifts from blue to yellow with the OT chain length increase. Compound **3a** exhibits spectroscopic and visual properties similar to those of **P** standard.

Our molecules, since quite stable towards temperature and chemical degradation, might be useful as fluorescent probes in biological applications as well as components in molecular devices for energy conversion. Therefore, because of their potential interest in the biological field, their fluorescence quantum yields have been estimated with samples diluted in DMSO at ambient conditions (Table 1 - Φ_F). Due to the large spectral span of our compounds, we used Perylene or Anthracene as actinometers. We used perylene standard (**P**) for compounds **4**, **4a**, **5** and **5a** and anthracene standard (**A**) for compounds **3**, **3a**, **6** and **6a**. UV absorption and fluorescence emission of both standards are shown in Figure SI1.

When compared to their nitrile precursors (**4**–**6**), compounds **4a, 5a** and **6a** display a significant red-shifted emission, indicative of an electronic distribution more delocalized over the OT chain and the DAT groups in agreement with the extended π-π conjugation (Fig. 3). Otherwise, Figure SI2 shows that no shift occurs between the fluorescence λ_{max} of compounds **3** and the DAT derivative **3a** ($\lambda_{max=}$442 nm), with an almost perfect overlap of the two transitions but much larger emission intensity of the DAT product (Table 1).

In the series of oligothiophenes bearing nitrile groups (**3**–**5**), the better electronic delocalization in the molecular structure and the fluorescence quantum yields went along with the displacement of

Please cite this article as: A.D. Rodrigues et al., Original synthesis and spectroscopic study of thiophene triazine derivatives with enhanced luminescence properties, Spectrochimica Acta Part A: Molecular and Biomolecular Spectroscopy, https://doi.org/10.1016/j.saa.2019.117708

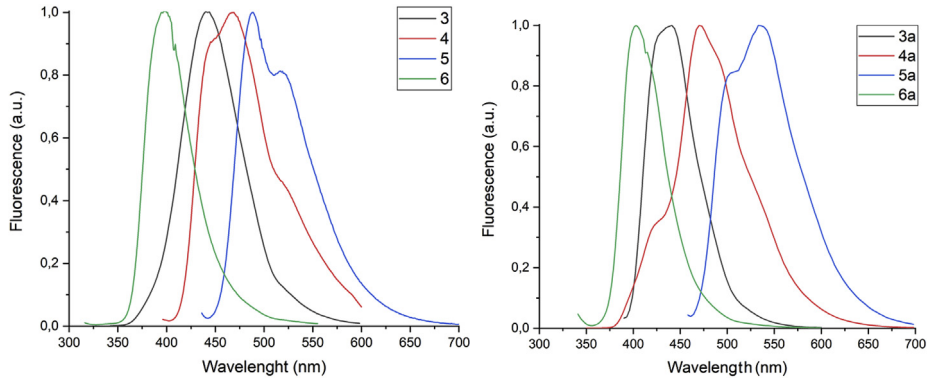

Fig. 3. Normalized emission spectra of derivatives **3**–**6** (left) and **3a-6a** (right) (air equilibrated DMSO solutions at T_{room}).

Table 1
UV-visible and fluorescence spectroscopic data for compounds 3–6 and their DAT derivatives 3a-6a in air equilibrated DMSO solutions. For compounds 3, 3a, 6 and 6a, Anthracene (A) in ethanol ($\Phi_F = 0.28 \pm 0.02$) [19] has been used as a standard for fluorescence quantum yields calculations. Perylene (P) in DMSO ($\Phi_F = 0.78 \pm 0.02$) [20] has been used for compounds 4, 4a, 5 and 5a. Stokes shifts are calculated from the difference between the emission λ_{max} and the excitation λ_0 converted in cm^{-1}. E_{00} transitions are obtained from the spectral position corresponding to the crossing of excitation and emission spectra (Fig. 2). *Eg* were optical estimates of the band gaps (see explanation in the text).

Compound	λ_{max} Absorption (nm) / ε (L. mol^{-1} cm^{-1})	Excitation wavelength (nm)	λ_{max} Emission (nm)	Stokes shift (cm^{-1})	E_{00}, (E_g) (eV)	Φ_F (±0.05)
3	346 / (9862)	342	442	6280	3.18 (3.6)	0.05
4	396 /(16905)	394	468	3885	2.85 (3.1)	0.41
5	431 / (25404)	422	488	2710	2.64 (2.9)	0.55
6	317 / (39921)	307	398	6420	3.40 (3.9)	0.18
3a	377 / (37909)	380	442	3900	3.3 (3.3)	0.78
4a	419 / (36196)	404	474	2770	2.76 (2.9)	0.59
5a	447 / (30151)	439	538	3785	2.55 (2.7)	0.26
6a	344 / (26628)	342	405	4380	3.26 (3.6)	0.22

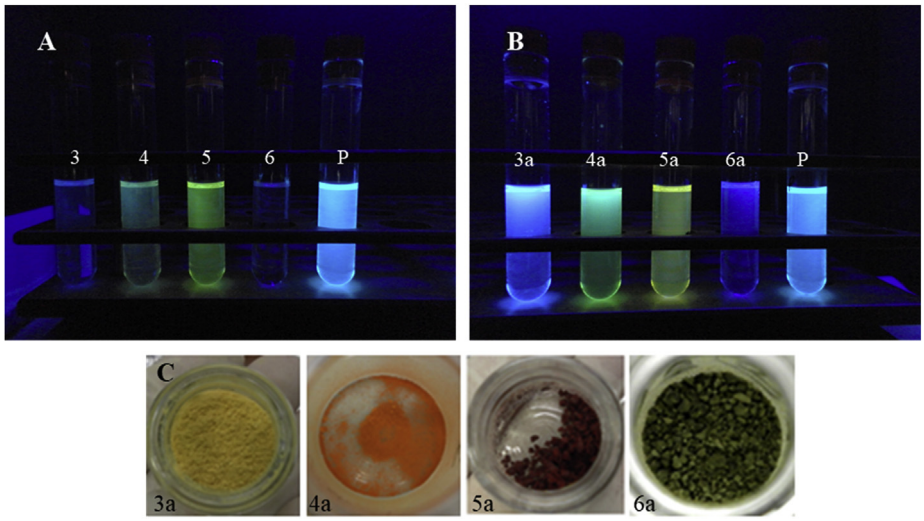

Fig. 4. **(A)** compounds **3**–**6** and standard **P** at 1.0×10^{-6} M in DMSO solutions irradiated with an UV lamp ($\lambda = 366$ nm); **(B) 3a-6a** and standard **P** at 1.0×10^{-6} M in DMSO solutions irradiated with an UV lamp ($\lambda = 366$ nm) and **(C) 3a-6a** at solid state in day-light.

the emission maxima wavelengths. The quantum efficiency increases with the OT chain length (($\Phi_F = 0.05 \pm 0.05$ for bithiophene (**3**), $\Phi_F = 0.41 \pm 0.05$ for terthiophene (**4**) and $\Phi_F = 0.55 \pm 0.05$ for quaterthiophene (**5**))). Otherwise, as previously observed for the molar absorptivity values (ε), the quantum efficiency of DAT derivatives (**3a**-**5a**) show the opposite behavior i.e. decrease of Φ_F with the increase of the OT chain length. This phenomenon is probably related to the formation of more constrained structures with lower degrees of torsional freedom.

Compound **3a** exhibits a highly efficient fluorescence emission, with a quantum yield $\Phi_F = 0.78 \pm 0.05$ resulting from the extended $\pi-\pi$ conjugation and, probably, the higher steric hindrance of such a small molecule. Similarly, compound **4a** shows good fluorescence emission properties with $\Phi_F = 0.59 \pm 0.05$ and green fluorescence brightness when irradiated with a UV light at 366 nm (Fig. 4).

Compound **5a** presents lower quantum yield $\Phi_F = 0.26 \pm 0.05$ when compared to the corresponding nitrile precursor **5** ($\Phi_F = 0.55 \pm 0.05$). However, the following interesting behavior was

Please cite this article as: A.D. Rodrigues et al., Original synthesis and spectroscopic study of thiophene triazine derivatives with enhanced luminescence properties, Spectrochimica Acta Part A: Molecular and Biomolecular Spectroscopy, https://doi.org/10.1016/j.saa.2019.117708

observed visually: fluorescence brightness changes from green-yellow to yellow when **5** is converted into **5b** (compare the related test tubes in Fig. 4-A and **4-B**), which is the hint of a slightly extended electronic delocalization in the molecular structure of the last compound. The antagonistic effect brought by the DAT groups in structure and fluorescence properties makes compound **5** behave similarly to compound **4a** i.e. greenish fluorescence brightness and close quantum yields ($\Phi_F = 0.55 \pm 0.05$ and $\Phi_F = 0.59 \pm 0.05$ respectively).

Contributions of the DAT function to the molecular structure of the samples (**3a**-**5a**) seem to induce an improved electronic delocalization and more rigid structures increasing the fluorescence quantum yield.

Compound **6** ($\Phi_F = 0.18 \pm 0.05$) shows a fluorescence quantum yield higher than **3** ($\Phi_F = 0.05 \pm 0.05$) but both display a large Stokes shift linked to a major change in the geometry of the excited state related to the ground state.

3. Conclusions

We report a straightforward access to π-conjugated oligothiophenes and phenylthiophenes bearing amino-rich groups. The compounds were synthesized using a palladium-catalyzed C–H arylation in the main step of the synthesis, leading to nitrile derivatives (**3**–**6**) in moderate to excellent yields. Further cycloaddition reactions with 2-cyanoguanidine led to DAT derivatives (**3a**-**6a**) in good to excellent yields. UV-Vis absorption and fluorescence studies were performed with all compounds to determine their basic spectroscopic properties. We have identified a strongly emissive molecule (compound **3a**) with fluorescence quantum yield $\Phi_F = 0.78 \pm 0.05$, which could find applications in biology and material chemistry. We have observed an antagonistic effect in the spectroscopic properties of oligothiophenes bearing DATs, resulting in more constrained structures with improved absorptive and emissive properties when decreasing the OT chain length. The spectroscopic study of this new family of compounds showed such differences in the absorption properties of the different molecules to preclude any global guess relative to their excited state property. Anyhow, some of these DAT substituted compounds have an actual potential interest as fluorescent labels while others might be of interest for the conception of molecular electronic devices.

4. Experimental

All reactions were carried out in anhydrous or freshly distillated solvents in oven dried Schlenk flasks under argon atmosphere or air (when not mentioned). Commercial reagents have been used without any further purification.

Analytical thin layer chromatography (TLC) was performed using Merck silica gel 60 F_{254} pre-coated plates. Chromatograms were observed under UV light at 254 nm and/or 366 nm. NMR spectroscopic data were obtained with a Bruker Advance 300 and 600 MHz and chemical shifts were quoted in parts per million (ppm) relative to residual solvent peak. *J* values are given in hertz. High performance liquid chromatography (HPLC) was performed on an Alliance 2795-Waters with mass spectrometry (MS) detection ESI-QTOF-Waters using electrospray ionization (ESI) or by direct introduction. GC-MS (QP2010 plus – Shimadzu) analyses were performed to follow the reactions depending on the polarity of the products. FTIR analyses were done with purified solid samples in the attenuated total reflectance (ATR) mode on a Vector22 Bruker equipment. Elemental analysis was performed on a FlashEA® 1112-Thermo equipment.

UV-Vis spectra were performed in a Lambda 35 double beam spectrophotometer (PerkinElmer), using DMSO (Sigma-Aldrich, 99.9%) as solvent and a scan speed of 120 nm min^{-1}. DMSO was chosen as solvent due to the lack of solubility of the DAT derivatives in other low toxicity solvent. Total dissolution of the samples was carefully checked before running the spectra. The molar extinction coefficients (ε) were calculated following precise controlled dilutions of mother solutions.

HOMO-LUMO energy gap (eV) was estimated directly from UV-Vis λ_{max} absorption according to $\mathbf{E_g} = \boldsymbol{h.c}\ /\lambda$ formula where ***h*** is Planck's constant (J.s), **c** is the speed of light (m/s) and **λ** is the absorption wavelength (nm), resulting (after conversion) in the simplified formula $\mathbf{E_g} = 1240/\lambda_{max}$.

Fluorescence studies were performed on a spectrofluorimeter (K2-001, ISS, Champaign, USA) running in the steady state mode and using a right-angle geometry. The instrument was fitted with a 300 W xenon short arc lamp (Excelitas Technologies' Cermax®) and single concave holographic grating monochromator with interchangeable slits ranging from 0.4 to 32 nm. Emission spectra were carried out using excitation wavelengths reported in Table 1 and all spectroscopic data relative to a given compound were measured using the same 1 cm Hellma fluorescence cell for absorption, excitation and emission.

Quantum yields were obtained by the relative method using optically dilute solutions (Abs. < 0.02), with samples at room temperature (23 °C ± 2 °C) in a dark room. Data are for air equilibrated samples and are not corrected from instrument response. Perylene (**P**) in DMSO and anthracene (**A**) in ethanol have been used as standards, with the respective literature values of $\Phi_F = 0.78 \pm 0.02$ for **P** in DMSO [19] and $\Phi_F = 0.28 \pm 0.02$ for **A** in ethanol [20], considering the differences in refractive indexes of solvents for analyzed samples (always in DMSO) and standards when necessary. Refractive index of DMSO (n = 1.4793) and ethanol (n = 1.3617) were used in the calculations. The relative fluorescence quantum yields were determined using the same cells, excitation wavelengths for emission spectra of samples and standards, same gain and slit bandwidths applying the following formula for the estimations:

$$\varphi = \varphi_{ref} \frac{I}{I_{ref}} \frac{1 - 10^{Aref}}{1 - 10^{A}} \frac{n^2}{n_{ref}^2}$$

where Φ and Φ_{ref} were the fluorescence quantum yields of the unknown sample and the respective reference, η and η_{ref} are the refractive indexes of the solvents used to dilute the samples and references, I and I_{ref} are the integrated fluorescence intensities of the samples and references respectively and A and A_{ref} are the absorbances at the excitation wavelengths of the samples and references respectively.

4.1. General procedure for the synthesis of 3–6

A mixture of aryl bromide (1 eq.), 2-thiophenecarbonitrile (3 eq. per site), K_2CO_3 (1.5 eq. per site), pivalic acid (0.15 eq. per site) and $Pd(PPh_3)_4$ (4 mol % per site) in a solvent mixture of dry N,*N*-dimethylacetamide/toluene 50:50 (v/v %), C:0.23 M, was stirred under argon atmosphere at 110 °C during 48h. The reaction mixture was then diluted with water, filtered on Celite and washed with diethyl ether. The solid was resolubilized in THF/diethyl ether 50:50 (v/v %) and centrifuged (15 min, 4000 rpm, rt). The white solid was eliminated and the solution evaporated to give a product which was purified by successive recrystallizations in appropriate solvents: **3**, **4** and **6** in 1-butanol and **5** in toluene at room temperature. Yields: (**3**) 35%, yellow solid; (**4**) 45%, orange solid; (**5**) 72%, red solid; (**6**) 93%, green solid. All amounts were calculated based on each reactive site (-Br) of the starting precursor.

[2.2′-bithiophene]-5.5′-dicarbonitrile (**3**): ^{1}H NMR (DMSO-d_6, 600 MHz.) δ (ppm): 8.02 (d, J = 4.18 Hz. 1H), 7.71 (d, J = 3.96 Hz. 1H), ^{13}C NMR (DMSO-d_6, 150 MHz.) δ (ppm): 141.2, 140.4, 127.2, 113.8, 108.6, GC-MS: m/z = 216.20, HRMS (ESI+): m/z = 216.9894, UV-*vis*

Please cite this article as: A.D. Rodrigues et al., Original synthesis and spectroscopic study of thiophene triazine derivatives with enhanced luminescence properties, Spectrochimica Acta Part A: Molecular and Biomolecular Spectroscopy, https://doi.org/10.1016/j.saa.2019.117708

(λ_{max}): 346 nm, IR (ATR cm^{-1}): 3093, 3073, 2215, 1594, 1480, 1430, 1295, 1151, 1058, 882, 809, 522.

[2,2':5′,2″-terthiophene]-5,5″-dicarbonitrile (**4**): ^{1}H NMR (DMSO-d_6, 600 MHz) δ (ppm): 7.95 (d, J = 3,96 Hz, 2H), 7.595 (s, 2H), 7.54 (d, J = 3.96 Hz, 2H), ^{13}C NMR (DMSO-d_6, 150 MHz) δ (ppm): 142.7, 140.2, 135.1, 128.1, 125.3, 113.9, 106.9, HRMS (ESI+): m/z = 297.9695, UV-*vis* (λ_{max}): 396 nm IR (ATR cm^{-1}): 3094, 3071, 2924, 2824, 2214, 1431, 1045, 806, 784.

[2,2':5′,2'':5″,2‴-quaterthiophene]-5,5‴-dicarbonitrile (**5**): ^{1}H NMR at 40 °C (DMSO-d_6, 600 MHz) δ (ppm): 7.94 (d, J = 3,8 Hz, 2H), 7.56 (d, J = 3.8 Hz, 2H), 7.51 (d, J = 3.8 Hz, 2H), 7.46 (d, J = 3.8 Hz, 2H), ^{13}C NMR at 40 °C (DMSO-d_6, 150 MHz) δ (ppm): 143.1, 140.1, 136.6, 133.4, 128.1, 126.3, 124.78, 113.9, 106.3, HRMS (ESI+): m/z = 380.9644, UV-*vis* (λ_{max}): 431 nm, IR (ATR cm^{-1}): 3094, 3078, 2215, 1542, 1446, 1433, 1047, 852, 789.

5,5′,5''-(benzene-1,3,5-triyl)tris(thiophene-2-carbonitrile) (**6**): ^{1}H NMR (DMSO-d_6 600 MHz) δ (ppm): 8.077 (s, 2H), 8.072 (s, 2H), 7.97 (d, J = 3.81 Hz, 2H), ^{13}C NMR (DMSO-d_6 150 MHz) δ (ppm): 148.8, 140.1, 133.9126.6124.5, 114.1, 108.0 HRMS (ESI+): m/z = 400.0037, UV-*vis* (λ_{max}): 317 nm, IR (ATR cm^{-1}): 3395, 3106, 2214, 1594, 1422, 1323, 1238, 1038, 807.

4.2. General procedure for the synthesis of ***3a-6a***

A mixture of the nitrile derivatives (**3**–**6**) (1 eq.), 2-cyanoguanidine (3 eq. per site) and KOH (1 eq. per site) in DMSO (C: 0.1 M) was stirred at 80 °C for 16h. Distilled water was added and the crude was recrystallized at 80 °C during 15 min. The precipitated solid was then hot filtrated on Celite, washed with acetonitrile and purified by recrystallizations in THF. Yields: **3(a)** 98%, yellow solid; (**4a)** 74%, orange solid; (**5a)** 91%, dark red solid; (**6a)** 77%, green solid. All amounts are calculated based on each reactive site (-CN) of the starting precursor.

6,6'-([2,2′-bithiophene]-5,5′-diyl)bis(1,3,5-triazine-2,4-diamine) (**3a**): ^{1}H NMR (DMSO-d_6, 600 MHz) δ (ppm): 7.77 (d, J = 3.96 Hz, 2H), 7.42 (d, J = 3.96 Hz, 2H), 6.71 (bs, 8H, NH_2), ^{13}C (DMSO-d_6, 150 MHz) δ (ppm): 166.9, 166.1, 142.3, 139.7, 129.6, 125.3, HRMS (ESI+): m/z = 385.0758, UV-*vis* (λ_{max}): 377 nm, IR (ATR cm^{-1}): 3329, 3166, 1644, 1499, 1424, 1379, 1027, 795, 574.

6,6'-([2,2':5′,2″-terthiophene]-5,5″-diyl)bis(1,3,5-triazine-2,4-diamine) (**4a**): ^{1}H NMR (DMSO-d_6, 600 MHz) δ (ppm): 7.75 (d, J = 3.81 Hz, 2H), 7.430 (s, 2H), 7.39 (d, J = 3.81 Hz, 2H), 6.78 (bs, 8H, $-NH_2$), ^{13}C NMR (DMSO-d_6, 150 MHz) δ (ppm): 166.9, 166.1, 141.8, 139.2, 135.9, 129.6, 126.1, 125.0, HRMS (ESI+): m/z = 467.0645, UV-*vis* (λ_{max}): 419 nm, IR (ATR cm^{-1}): 3454, 3316, 3121, 1614, 1515, 1429, 1382, 1013, 794.

6,6'-([2,2':5′,2'':5″,2‴-quaterthiophene]-5,5‴-diyl)bis(1,3,5-triazine-2,4-diamine) (**5a**): ^{1}H NMR (DMSO-d_6 600 MHz) δ (ppm): 7.75 (d, J = 3.81 Hz, 2H), 7.42 (d, J = 3.81 Hz, 2H), 7.38 (m, J = 6.74 Hz, 4H), 6.77 (bs, 8H, $-NH_2$), ^{13}C NMR (DMSO-d_6 150 MHz) δ (ppm): 166.9, 166.1, 141.7, 139.3, 135.5, 135.4, 129.7, 126.0, 125.7, 124.9, HRMS (ESI+): m/z = 549.0527, UV-*vis* (λ_{max}): 447 nm, IR (ATR cm^{-1}): 3324, 3153, 1622, 1524, 1429, 1386, 848.

6,6′,6''-(benzene-1,3,5-triyltris(thiophene-5,2-diyl)) tris(1,3,5-triazine-2,4-diamine) (**6a**): ^{1}H NMR (DMSO-d_6 600 MHz) δ (ppm): 7.96 (s, 2H), 7.85 (d, J = 3.81 Hz, 2H), 7.81 (d, J = 3.81 Hz, 2H), 6.78 (bs, 8H, $-NH_2$), ^{13}C NMR (DMSO-d_6 150 MHz) δ (ppm): 168.4, 167.6, 146.7, 144.2, 136.7, 131.1, 127.2, 123.3, HRMS (ESI+): m/z = 652,1349, UV-*vis* (λ_{max}): 344 nm, IR (ATR cm^{-1}): 3326, 3154, 1633, 1518, 1461, 1423, 1384, 863, 797.

Declaration of competing interests

The authors declare that they have no known competing financial interests or personal relationships that could have appeared to influence the work reported in this paper.

Acknowledgments

The authors would like to thank the "Ministère de l'Éducation Nationale, de l'Enseignement Supérieur et de la Recherche" (MENESR) and The "Ecole Nationale Supérieure de Chimie de Montpellier" (ENSCM) for supporting this work.

Note: The authors declare no competing financial interest.

Appendix A. Supplementary data

Supplementary data to this article can be found online at https://doi.org/10.1016/j.saa.2019.117708.

References

[1] M.B. Zaman, D.F. Perepichka, A new simple synthesis of poly(thiophene-methine)s, Chem. Commun. (J. Chem. Soc. Sect. D) (33) (2005) 4187–4189, https://doi.org/10.1039/b506138e.

[2] K.R.J. Thomas, Y.-C. Hsu, J.T. Lin, K.-M. Lee, K.-C. Ho, C.-H. Lai, Y.-M. Cheng, P.-T. Chou, 2,3-disubstituted thiophene-based organic dyes for solar cells, Chem. Mater. 20 (5) (2008) 1830–1840, https://doi.org/10.1021/cm702631r.

[3] Y.M. Sun, Y.Q. Liu, Y.Q. Ma, C.A. Di, Y. Wang, W. Wu, G. Yu, W.P. Hu, D.B. Zhua, Organic thin-film transistors with high mobilities and low operating voltages based on 5,5 '-bis-biphenyl-dithieno[3,2-b : 2 ',3 '-d]thiophene semiconductor and polymer gate dielectric, Appl. Phys. Lett. (24) (2006) 88, https://doi.org/10.1063/1.2209213.

[4] Y.M. Sun, Y.Q. Ma, Y.Q. Liu, Y.Y. Lin, Z.Y. Wang, Y. Wang, C.A. Di, K. Xiao, X.M. Chen, W.F. Qiu, B. Zhang, G. Yu, W.P. Hu, D.B. Zhu, High-performance and stable organic thin-film transistors based on fused thiophenes, Adv. Funct. Mater. 16 (3) (2006) 426–432, https://doi.org/10.1002/adfm.200500547.

[5] H. Ahn, J.E. Whitten, Optical and electronic properties of electron polymerized thiophene films, Abstr. Pap. Am. Chem. Soc. 222 (2001). U288-U288.

[6] M.L. Capobianco, G. Barbarella, A. Manetto, Oligothiophenes as fluorescent markers for biological applications, Molecules 17 (1) (2012) 910–933, https://doi.org/10.3390/molecules17010910.

[7] A. Åslund, C.J. Sigurdson, T. Klingstedt, S. Grathwohl, T. Bolmont, D.L. Dickstein, E. Glimsdal, S. Prokop, M. Lindgren, P. Konradsson, D.M. Holtzman, P.R. Hof, F.L. Heppner, S. Gandy, M. Jucker, A. Aguzzi, P. Hammarström, K.P.R. Nilsson, Novel pentameric thiophene derivatives for in vitro and in vivo optical imaging of a plethora of protein aggregates in cerebral amyloidoses, ACS Chem. Biol. 4 (8) (2009) 673–684, https://doi.org/10.1021/cb900112v.

[8] D. Kok, M.A. Húngaro Duarte, R. Abreu Da Rosa, M.H. Wagner, J.R. Pereira, M.V. Reis Só, Evaluation of epoxy resin sealer after three root canal filling techniques by confocal laser scanning microscopy, Microsc. Res. Tech. 75 (9) (2012) 1277–1280, https://doi.org/10.1002/jemt.22061.

[9] T. Jando, K. Mori, Cross-linking of poly(vinyl chloride) fibers with 2-dibutylamino-4,6-dimercapto-1,3,5-triazine in water, Polym. J. 22 (9) (1990) 793–802, https://doi.org/10.1295/polymj.22.793.

[10] F. Saczewski, A. Bułakowska, P. Bednarski, R. Grunert, Synthesis, structure and anticancer activity of novel 2,4-diamino-1,3,5-triazine derivatives, Eur. J. Med. Chem. 41 (2) (2006) 219–225, https://doi.org/10.1016/j.ejmech.2005.10.013.

[11] K. Grossmann, S. Tresch, P. Plath, Triaziflam and diaminotriazine derivatives affect enantioselectively multiple herbicide target sites, Z. Naturforschung. C-a. J. Biosci. 56 (7-8) (2001) 559–569.

[12] W.C. Song, X.K. Xu, Q. Chen, Z.Z. Zhuang, X.H. Bu, Nitrogen-rich diaminotriazine-based porous organic polymers for small gas storage and selective uptake, Polym. Chem. 4 (17) (2013) 4690–4696, https://doi.org/10.1039/C3PY00590A.

[13] M. Mastalir, B. Stöger, E. Pittenauer, G. Allmaier, K. Kirchner, Air-stable triazine-based Ni(II) PNP pincer complexes as catalysts for the suzuki-miyaura cross-coupling, Org. Lett. 18 (13) (2016) 3186–3189, https://doi.org/10.1021/acs.orglett.6b01398.

[14] T. Imberdis, A. Ayrolles-Torro, A.D. Rodrigues, J. Torrent, M.T. Alvarez-Martinez, G.G. Kovacs, J.-M. Verdier, M. Robitzer, V. Perrier, A Fluorescent Oligothiophene-Bis-Triazine ligand interacts with PrP fibrils and detects SDS-resistant oligomers in human prion diseases, Mol. Neurodegener. 11 (2016) 1–19, https://doi.org/10.1186/s13024—016-0074-7.

[15] M.M.M. Raposo, A.M.C. Fonseca, G. Kirsch, Synthesis of donor-acceptor substituted oligothiophenes by Stille coupling, Tetrahedron 60 (18) (2004) 4071–4078, https://doi.org/10.1016/j.tet.2004.03.022.

[16] D. Lapointe, K. Fagnou, Overview of the mechanistic work on the concerted metallation-deprotonation pathway, Chem. Lett. 39 (11) (2010) 1119–1126, https://doi.org/10.1246/cl.2010.1118.

[17] M. Lafrance, K. Fagnou, Palladium-catalyzed benzene arylation: incorporation of catalytic pivalic acid as a proton shuttle and a key element in catalyst design, J. Am. Chem. Soc. 128 (51) (2006) 16496–16497, https://doi.org/10.1021/ja067144j.

[18] A.D. Rodrigues, T. Imberdis, V. Perrier, M. Robitzer, Improved synthesis of a quaterthiophene-triazine-diamine derivative, a promising molecule to study pathogenic prion proteins, Tetrahedron Lett. 56 (2) (2015) 368–373, https://doi.org/10.1016/j.tetlet.2014.11.098.

Please cite this article as: A.D. Rodrigues et al., Original synthesis and spectroscopic study of thiophene triazine derivatives with enhanced luminescence properties, Spectrochimica Acta Part A: Molecular and Biomolecular Spectroscopy, https://doi.org/10.1016/j.saa.2019.117708

[19] K. Suzuki, A. Kobayashi, S. Kaneko, K. Takehira, T. Yoshihara, H. Ishida, Y. Shiina, S. Oishi, S. Tobita, Reevaluation of absolute luminescence quantum yields of standard solutions using a spectrometer with an integrating sphere and a back-thinned CCD detector, Phys. Chem. Chem. Phys. 11 (42) (2009) 9850–9860, https://doi.org/10.1039/b912178a.

[20] Q.H. Zhou, M. Zhou, Y. Wei, X. Zhou, S. Liu, S. Zhang, B. Zhang, Solvent effects on the triplet-triplet annihilation upconversion of diiodo-Bodipy and perylene, Phys. Chem. Chem. Phys. 19 (2) (2017) 1516–1525, https://doi.org/10.1039/c6cp06897a.

[21] A.S. Bhadwal, R.M. Tripathi, R.K. Gupta, N. Kumar, R.P. Singh, A. Shrivastav, Biogenic synthesis and photocatalytic activity of CdS nanoparticles, RSC Adv. 4 (2014) 9484–9490, https://doi.org/10.1039/c3ra46221.

[22] J.C.S. Costa, R.J.S. Taveira, C.F.R.A.C. Lima, A. Mendes, L.M.N.B.F. Santos, Optical band gaps of organic semiconductor materials, Opt. Mater. 58 (2016) 51–60, https://doi.org/10.1016/j.optmat.2016.03.041.

[23] J. Sworakowski, How accurate are energies of HOMO and LUMO levels in small-molecule organic semiconductors determined from cyclic voltammetry or optical spectroscopy? Synth. Met. 235 (2018) 125–135, 10.1016.013.

Please cite this article as: A.D. Rodrigues et al., Original synthesis and spectroscopic study of thiophene triazine derivatives with enhanced luminescence properties, Spectrochimica Acta Part A: Molecular and Biomolecular Spectroscopy, https://doi.org/10.1016/j.saa.2019.117708